CD106/VCAM-1 distinguishes a fibroblast subpopulation with high colony-forming capacity and distinct protein expression from the uterosacral ligament

Yizhen Sima[1,2,3,4#], Junwei Li[1#], Chengzhen Xiao[1], Leimei Xu[1], Ling Wang[2,3,4], Yisong Chen[1]

[1]Department of Gynecology, Obstetrics and Gynecology Hospital of Fudan University, Shanghai, China; [2]Laboratory for Reproductive Immunology, Obstetrics and Gynecology Hospital of Fudan University, Shanghai, China; [3]Shanghai Key Laboratory of Female Reproductive Endocrine-Related Diseases, Shanghai, China; [4]The Academy of Integrative Medicine of Fudan University, Shanghai, China

Contributions: (I) Conception and design: Y Sima, Y Chen; (II) Administrative support: L Wang, Y Chen, J Li; (III) Provision of study materials or patients: J Li, C Xiao, L Xu; (IV) Collection and assembly of data: Y Sima; (V) Data analysis and interpretation: Y Sima, Y Chen; (VI) Manuscript writing: All authors; (VII) Final approval of manuscript: All authors.

[#]These authors contributed equally to this work.

Correspondence to: Yisong Chen. Department of Gynecology, Obstetrics and Gynecology Hospital of Fudan University, Shanghai 200011, China. Email: 123910566@qq.com; Ling Wang. Laboratory for Reproductive Immunology, Obstetrics and Gynecology Hospital of Fudan University, Shanghai 200011, China. Email: Dr.wangling@fudan.edu.cn.

Background: Pelvic organ prolapse (POP) is a common degenerative disease in women which may diminish quality of life. Investigating the pathological changes of the uterosacral ligament, including the functional changes of fibroblasts, is critical to understanding the pathophysiology of POP. This study was designed to isolate CD106-positive ($CD106^+$) fibroblasts from the human uterosacral ligament and assess the function and expression of this subpopulation.

Methods: We separated $CD106^+$ fibroblasts and CD106 negative ($CD106^-$) fibroblasts by fluorescence-activated cell sorting (FACS) and cultured them for subsequent experiments. Flow cytometric analysis was used to test the sorting efficiency, CD106 expression, and typical mesenchymal stem cell (MSC) phenotype marker expression. A colony-forming unit (CFU) assay was applied to evaluate the colony-forming ability of the fibroblasts. Trilineage differentiation capacities were assessed after *in vitro* induction. The protein levels of vimentin, fibroblast specific protein-1 (FSP-1), collagen I (COL 1), matrix metallopeptidase-1 (MMP-1), and α-smooth muscle actin (α-SMA) were detected by western blot analysis. The expression of CD106 was verified by flow cytometric analysis and immunohistochemistry (IHC) in the POP and non-POP groups.

Results: The $CD106^+$ fibroblasts were isolated with a purity of (93.50±3.91)%. The $CD106^+$ fibroblasts exhibited higher colony-forming capacity than that of $CD106^-$ fibroblasts, but neither of them showed adipogenic or osteogenic differentiation similar to that of MSCs. The protein levels of MMP-1 and α-SMA were lower, and the level of COL 1 was higher in the $CD106^+$ fibroblasts than in the CD106– fibroblasts. In addition, we observed a decreased expression of CD106 in the POP group compared with the non-POP group.

Conclusions: Our results suggest that $CD106^+$ fibroblasts possess a high colony-forming capacity and distinct protein expression, and this subpopulation is reduced in POP.

Keywords: Fibroblasts; CD106; uterosacral ligament; pelvic organ prolapse (POP)

Submitted Sep 27, 2021. Accepted for publication Jan 28, 2022.
doi: 10.21037/atm-21-5136
View this article at: https://dx.doi.org/10.21037/atm-21-5136

Introduction

Pelvic organ prolapse (POP) is the herniation of pelvic organs into the vagina caused by the weakening of pelvic floor supportive tissues. On examination, up to 50% of parous women have some degree of POP (1). Although many risk factors, such as age, parity, chronic cough, obesity, and constipation, are relevant to POP (2), the exact pathogenesis mechanisms of POP remain poorly understood, which impedes the development of treatments. To explore the etiology and pathophysiology of POP, we must understand the pathological changes of the uterosacral ligament, which is one of the primary suspensory structures providing apical support to the uterus and vagina (3).

Fibroblasts are the most abundant cell type in the uterosacral ligament and regulate the homeostasis of the extracellular matrix (ECM). Dysregulation of the ECM has been associated with altered connective tissue turnover in POP. The expressions of collagen and elastin, and proteins involved in their metabolism have been reported in POP (4-6). These proteins determine the mechanical properties and integrity of connective tissues; therefore, altered ECM homeostasis contributes to the development of POP.

Fibroblasts isolated from the uterosacral ligaments or vaginal wall have been intensively investigated to elucidate the pathophysiology of POP. Pathological changes in fibroblasts, such as an increase in intracellular reactive oxygen species and abnormal ECM production, have been observed under the mechanical stress of POP (7-10). Fibroblasts are recognized as a heterogeneous population of cells in several organs and tissues (11). The FSP1-positive fibroblasts exhibit a proangiogenic function in wound healing (12), and multiple subtypes of fibroblasts have been found to play different roles in lung fibrosis (13,14). However, we lack comprehensive knowledge of the heterogeneity of this pivotal cell type in POP. Recently, a high-throughput single-cell transcriptomic study identified 7 fibroblast subtypes in the human vaginal wall (15), indicating that discovering the heterogeneity of fibroblasts and studying the function of each subtype are important to understanding the pathophysiology of POP more precisely.

Also known as vascular cell adhesion molecule-1 (VCAM-1), CD106 is a member of the immunoglobulin superfamily of proteins and is predominantly expressed in endothelial cells, where it mediates the rolling and adhesion of leukocytes (16). It has also been identified as a surface marker of mesenchymal stem cells (MSCs) and found to be expressed in 30–79% of human bone marrow-derived MSCs (BM-MSCs) (17,18). Previous studies have reported that $CD106^+$ MSCs have enhanced multipotency (19,20) and immunosuppressive activity (17,21,22), and that $CD106^+$ cardiac fibroblasts have lymphangiogenic capacity (23). In addition, CD106 has been reported as one of the differently expressed markers between fibroblasts and MSC, although most MSC markers are also expressed on fibroblasts (24,25). We also found that fibroblasts derived from the uterosacral ligament expressed similar surface markers to BM-MSC, except for CD106. Considering the importance of CD106 for MSC and the differential expression between MSC and fibroblasts, we sorted $CD106^+$ fibroblasts and explored if they were a novel MSC-like subpopulation in the human uterosacral ligament.

The objective of this study was to isolate $CD106^+$ fibroblasts from the human uterosacral ligament and assess the function and expression of this subpopulation. We successfully isolated $CD106^+$ fibroblasts and found that this subpopulation exhibited a high colony-forming capacity and increased collagen I (COL 1) expression, suggesting that $CD106^+$ fibroblasts are a subtype of uterosacral ligament fibroblasts. In addition, we found decreased expression of CD106 in both tissues and cultured fibroblasts from patients with POP, implying that changes in $CD106^+$ fibroblasts play a role in the pathophysiology of POP. This study elucidates the heterogeneity and functions of uterosacral ligament fibroblasts in POP. We present the following article in accordance with the MDAR reporting checklist (available at https://atm.amegroups.com/article/view/10.21037/atm-21-5136/rc).

Methods

Patients and sample collection

All procedures performed in this study involving human participants were in accordance with the Declaration of Helsinki (as revised in 2013). The study was approved by the Ethics Committee of the Obstetrics and Gynecology Hospital of Fudan University (No. 2017-12), and informed consent was taken from all the patients.

This study included 20 women who underwent hysterectomy for POP or other benign diseases in the Obstetrics and Gynecology Hospital of Fudan University. We assigned 10 patients who were diagnosed with stage III POP or greater (according to the pelvic organ prolapse quantification, POP-Q) to the POP group. The remaining 10, who underwent hysterectomy for other conditions,

Table 1 Patient characteristics

Characteristic	POP (n=10)	non-POP (n=10)	P value
Age (mean ± SD)	54.6±6.6	55.7±7.8	NS[†]
BMI (mean ± SD)	24.92±2.08	24.49±3.42	NS[†]
Parity (median, range)	1.2 (1–3)	1 (1–2)	NS[‡]
Menopause (n, %)	7 (70.0)	6 (60.0)	NS[§]
POP stage (median, range)	3 (3–4)	0	<0.05[‡]

[†], *t*-test; [‡], Mann-Whitney test; [§], Fisher's exact test. POP, pelvic organ prolapse; SD, standard deviation; NS, not significant; BMI, body mass index.

including hysteromyoma, adenomyosis, and high-grade squamous intraepithelial lesion, were assigned to the non-POP group. Clinical characteristics, including age, body mass index (BMI), parity, and menopausal status, were matched between the 2 groups (*Table 1*). None of the participants had a history of pelvic operations, pelvic inflammation, malignant diseases, serious systemic diseases, or hormone replacement therapy (HRT).

A 1 cm^2 piece of the uterosacral ligament was collected with a complete cross-section after hysterectomy. The sample tissues were cut into 2 pieces under aseptic conditions and prepared for cell culture or immunohistochemistry (IHC).

Culture of cells

We purchased human BM-MSCs from Cyagen Bioscience Inc. (Guangzhou, China). Human BM-MSC basal medium (Cyagen) supplemented with 1% penicillin-streptomycin (Cyagen), 1% glutamine, and 10% qualified fetal bovine serum (FBS; Cyagen) was used for BM-MSC culture. Cells were cultured at 37 ℃ in a 5% CO_2 atmosphere. The BM-MSCs were fed fresh medium every 2 days and detached by 0.25% trypsin, 0.04% ethylenediamine tetraacetic acid (EDTA) at 80–90% confluence. Cells from passages 3 to 5 were used in the following studies.

Human fibroblasts derived from the uterosacral ligaments were isolated and cultured as follows. The excised and fresh uterosacral ligament tissues were washed 3 times with sterile phosphate-buffered saline (PBS) containing 1% penicillin, streptomycin, and amphotericin B (Genom, Jiaxing, China) for 5 minutes and then cut into 1 mm^3 fragments. Then, the tissues were digested at 37 ℃ for 1 hour in PBS containing 0.2% collagenase type I (Sigma-Aldrich, St. Louis, MO, USA). After separation, the cells were cultured in Dulbecco's modified Eagle medium (DMEM), with 10% FBS (Gibco, Grand Island, NY, USA) and 1% penicillin-streptomycin-amphotericin B. The culture medium was replaced every 2 days. Cells were passaged at 80–90% confluence, and cells from passages 3 to 6 were used for the following experiments.

Colony-forming unit (CFU) assays

Human fibroblasts were harvested and passaged in 6-well plates at a density of 10 cells/cm^2. The fibroblasts were cultured in DMEM supplemented with 20% FBS for 10 days. The culture medium was renewed every 3 days. Next, the culture medium was removed, and the fibroblasts were washed twice with PBS. Then, 4% paraformaldehyde was used for cell fixation. After 20 minutes of fixation, the cells were washed and stained with crystal violet (Beyotime, Shanghai, China) for 30 minutes at room temperature. Cell colonies containing more than 50 cells were counted, and the total number of cell colonies was recorded in each group using a light microscope (Nikon, Tokyo, Japan).

Flow cytometry analysis

Fibroblasts were detached and washed with PBS supplemented with 2% FBS. A total of 2.5×10^5 cells in each sample were stained with antibodies for 20–30 minutes in the dark at room temperature. After being washed twice with PBS supplemented with 2% FBS, the cells were resuspended in 500 μL PBS and passed through a 100 mm nylon sieve. Flow cytometry [Becton Dickinson and Co. (BD), Franklin Lakes, NJ, USA] was used to analyze the cell samples. The antibodies used are listed in *Table 2*. Data were analyzed by FlowJo version X.0.7 (TreeStar, Ashland, OR, USA) (https://www.flowjo.com/solutions/flowjo/downloads). The number of positive cells relative to unstained cells, which were set as negative controls, was determined.

Fluorescence-activated cell sorting (FACS)

Passage 3 fibroblasts were harvested and stained using anti-human CD106 antibody (*Table 2*) as mentioned above. Cells were washed and resuspended in PBS supplemented with 2% FBS. With the aid of a BD FACSAria II cell sorter (BD), fibroblasts were separated into $CD106^+$ and $CD106^-$ cell populations. The sorted cells were washed with PBS and

Table 2 Antibodies used in this study

Antibody	Host/isotype	Application	Company	Dilution
FITC anti-human CD90	Mouse IgG1	FACS	Biolegend	1:20
FITC anti-human CD73	Mouse IgG1	FACS	Biolegend	1:20
FITC anti-human CD45	Mouse IgG1	FACS	Biolegend	1:20
FITC anti-human HLA-DR	Mouse IgG2a	FACS	Biolegend	1:20
PE anti-human CD105	Mouse IgG1	FACS	Biolegend	1:20
FITC anti-human CD34	Mouse IgG1	FACS	Biolegend	1:20
APC anti-human CD146	Mouse IgG1	FACS	Biolegend	1:20
APC anti-human CD106	Mouse IgG1	FACS	Biolegend	1:20
PE/Cyanine7 anti-human CD106	Mouse IgG1	FACS	Biolegend	1:20
Anti-human vimentin	Rabbit IgG	WB	Cell Signaling Technology	1:1,000
Anti-human collagen type I	Rabbit IgG	WB	Abcam	1:1,000
Anti-human α-SMA	Rabbit IgG	WB	Cell Signaling Technology	1:1,000
Anti-human S100A4/FSP-1	Rabbit IgG	WB	Abcam	1:1,000
Anti-human CD106/VCAM-1	Rabbit IgG	IHC	Abcam	1:200
Anti-human MMP-1	Rabbit IgG	WB	Abcam	1:1,000
Anti-human GAPDH	Rabbit IgG	WB	Abcam	1:3,000
HRP goat anti-rabbit IgG	Goat IgG	WB	Abcam	1:3,000

FITC, fluorescein isothiocyanate; FACS, fluorescence-activated cell sorting; HLA-DR, human leukocyte antigen-DR; PE, phycoerythrin; APC, allophycocyanin; WB, western blotting; α-SMA, α-smooth muscle actin; FSP-1, fibroblast specific protein-1; VCAM-1, vascular cell adhesion molecule-1; IHC, immunohistochemistry; MMP-1, matrix metallopeptidase-1; GAPDH, glyceraldehyde-3-phosphate dehydrogenase.

seeded onto 6-well plates at a density of 10 cells/cm^2 (for colony-forming assays) or 500 cells/cm^2 (for differentiation assays and subsequent long-term culture). Culture conditions were as described above.

Western blotting analysis

Radioimmunoprecipitation assay (RIPA) lysis buffer (Beyotime) was used to extract the total protein. After the protein was prepared, protein concentrations were measured using a bicinchoninic acid (BCA) kit (Beyotime). The proteins were denatured and separated by sodium dodecyl sulfate-polyacrylamide gel electrophoresis (SDS-PAGE). Next, the proteins located in the gels were transferred to polyvinylidene fluoride (PVDF) membranes, which were blocked by incubation with 5% bovine serum albumin (BSA; Sigma-Aldrich, St. Louis, MO, USA) or 5% nonfat-dried milk/tris-buffered saline with Tween (TBST) for 1 hour at room temperature. The primary antibodies were diluted according to the manufacturer's instructions. Then, the membranes were incubated with the primary antibodies overnight at 4 ℃. Next, the membranes were washed with TBST 3 times and incubated with the secondary antibody for 1 hour at room temperature. After being washed 3 times, the membranes were incubated with enhanced chemiluminescence reagent (Millipore, Billerica, MA, USA). The relative intensities of the protein bands to the internal reference bands were analyzed using analysis software [ImageJ 1.40g, National Institutes of Health (NIH), Bethesda, MD, USA].

In vitro differentiation

In vitro differentiation assays were performed in MSCs, CD106$^+$, and CD106$^-$ fibroblasts to evaluate the multi-differentiation potential. For osteogenic and adipogenic differentiation, the cells were cultured at a density of 500 cells/cm^2 in 6-well culture plates. After achieving 100% or 60% confluence, the medium was replaced with

adipogenic or osteogenic induction medium according to the instructions of the differentiation kit (Cyagen). After a 3-week culture, the potential of the cells to differentiate into an osteogenic or adipogenic lineage was assessed by staining the cells using Alizarin Red and Oil Red O solutions.

For chondrocyte differentiation, cells were detached and counted. The medium was replaced with an induction medium according to the instructions of the chondrogenic differentiation kit (Cyagen). Aliquots of 3×10^5 cells were placed in 15 mL centrifuge tubes and centrifuged to obtain pelleted cells. Then, 3 mL chondrogenic induction medium was gently added to the tubes to avoid resuspending the pelleted cells. After 24 hours of incubation, the cells formed a cell aggregate that did not adhere to the wall of the tube. The culture medium was carefully replaced every 2 days, and the cell aggregates were collected after 3 weeks of incubation. Then, the cell aggregates were made into paraffin sections and stained using Alcian Blue.

IHC

Hematoxylin-eosin (H&E) staining was performed to observe the morphology of the tissue, and IHC was used to compare CD106 expression between the POP and control groups. Tissue samples were fixed with 4% paraformaldehyde and were made into 4-μm thick paraffin sections. After deparaffinization, rehydration, antigen retrieval, and serum blocking, the paraffin sections were incubated with diluted primary antibodies and then with the secondary antibody. Subsequently, a 3,3'-diaminobenzidine (DAB) color developing solution was used to stain the sections, and a hematoxylin stain solution was used to counterstain the nuclei. Images were observed under a light microscope, and the area percentage of CD106-positive cells was calculated using the ImageJ software (ImageJ 1.40g, NIH).

Statistical analysis

Data were presented as the mean ± standard deviation (SD). A *t*-test was utilized to determine significant differences between the 2 groups when the data were normally distributed with equal SDs. A Mann-Whitney test was used when the data were not normally distributed. One-way analysis of variance (ANOVA) with Tukey's post hoc analysis was used for multiple comparisons. Differences between the 2 compared groups were considered statistically significant when $P<0.05$. All tests in the present study were performed using the software GraphPad Prism 8.0.2 (GraphPad Inc., San Diego, CA, USA).

Results

Human uterosacral ligament fibroblasts were sorted into CD106$^+$ and CD106$^-$ subpopulations

Primary human fibroblasts isolated from the uterosacral ligament were expanded and sorted into CD106$^+$ (4.14%±0.47%) and CD106$^-$ (87.60%±3.04%) subpopulations (*Figure 1A*). There was no morphological difference between the positive and negative cells, and they both exhibited a flat, spindle-shaped morphology typical of fibroblasts (*Figure 1B*). The efficiency of the cell sorting was verified by flow cytometry analysis (*Figure 1C*). The CD106$^+$ cells made up 93.50%±3.91%, 1.23%±0.53%, and 5.37%±2.32% of the CD106$^+$, CD106$^-$, and unsorted fibroblasts, respectively. To examine the expression of CD106 during the culture and expansion of the cells, we analyzed the positive cell numbers at passage 3 (cell sorting), passage 4, and passage 5. We found that the CD106$^+$ cell number decreased from 93.50%±3.91% to 47.37%±4.71% after 1 cell propagation (*Figure 1D*), so we chose passage 3 cells for further experiments. The data shown are the means ± SD of 3 independent experiments.

CD106$^+$ fibroblasts exhibited a higher colony-formation capacity

A series of typical surface markers of MSCs were examined by *in vitro* cultivation, including CD34, CD45, CD73, CD90, CD105, HLA-DR, and CD106. The fibroblasts exhibited the same expression pattern as MSCs in CD34, CD45, CD73, CD90, CD105, and HLA-DR (*Figure 2A*). However, the positive rate of CD106 was 35.6%±3.59% in MSCs compared to 4.2%±0.18% in uterosacral ligament fibroblasts (*Figure 2B*). We hypothesized that CD106$^+$ fibroblasts might be a novel MSC-like subpopulation in the human uterosacral ligament. To test this hypothesis, the CD106$^+$ cells and CD106$^-$ cells were cultured and subjected to a CFU assay, a test used to identify MSCs and reflect their self-renewal capacity. Significantly, compared with CD106$^-$ fibroblasts, CD106$^+$ fibroblasts possessed a 4-fold increased potential for colony formation, and unsorted fibroblasts exhibited a colony-formation ability similar to that of CD106$^-$ cells (*Figure 3*).

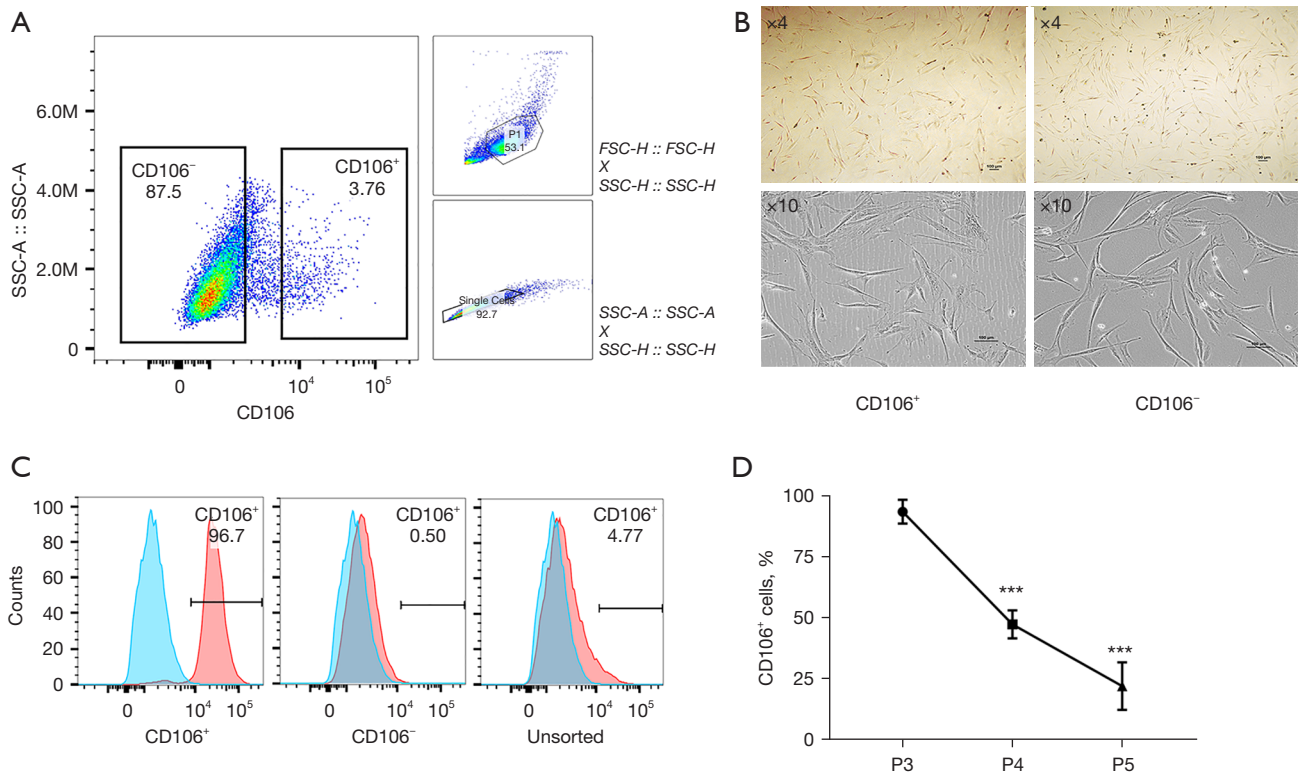

Figure 1 Isolation of CD106⁺ and CD106⁻ human uterosacral ligament fibroblasts. (A) CD106⁺ fibroblasts and CD106⁻ fibroblasts were sorted by FACS. Viable cells were selected by their FSC versus their SSC profile and single cells were selected by their height versus SSC-A. (B) Morphology of CD106⁺ fibroblasts and CD106⁻ fibroblasts, scale bar, 100 μm. Cultured cells were observed by an inverted microscope at low magnification (×4) and medium magnification (×10). (C) Flow cytometry analysis of CD106⁺ fibroblasts, CD106⁻ fibroblasts, and the unsorted fibroblasts. The blue areas represent unstained cells serving as controls; the red areas represent stained cells; the percentages of positively labeled cells are listed. (D) The percentage of CD106 positive cells in CD106⁺ fibroblasts during passaging (P3, P4, P5), P: passage. The data shown are the means ± SD of 3 independent experiments. ***, P<0.001 compared with CD106⁺ fibroblasts at P3. FACS, fluorescence-activated cell sorting; FSC, forward scatter; SSC, side scatter; SSC-A, side scatter-area; SSC-H, side scatter-height; FSC-H, forward side scatter-height; SD, standard deviation.

CD106⁺ fibroblasts did not exhibit multipotential differentiation capacity

To address our hypothesis that CD106⁺ fibroblasts are MSC-like cells, we compared the multilineage differentiation potential between MSCs, CD106⁺ fibroblasts, and CD106⁻ fibroblasts. For adipogenic differentiation, both types of fibroblasts exhibited few lipid droplets without a significant difference in Oil Red O staining. In contrast, the MSCs exhibited many positively stained lipid droplets (*Figure 4A*). For osteogenic differentiation, mineralization was qualitatively demonstrated by Alizarin Red staining, and neither of the fibroblast populations exhibited positive staining (*Figure 4B*). For chondrogenic differentiation, the cells exhibited positive staining by Alcian Blue, which stains the acidic mucopolysaccharide of the cartilage tissue (*Figure 4C*).

Differential expression of fibroblast typical proteins was observed in CD106⁺ fibroblasts

To explore the cell function of CD106⁺ fibroblasts, we detected the specific fibroblast proteins by western blot analysis (*Figure 5*). The fibroblast biomarkers vimentin and fibroblast specific protein-1 (FSP-1) were expressed on all cells, and there was no significant difference in their expressions between CD106⁺ and CD106⁻ fibroblasts. The expression levels of COL 1 and matrix metallopeptidase-1

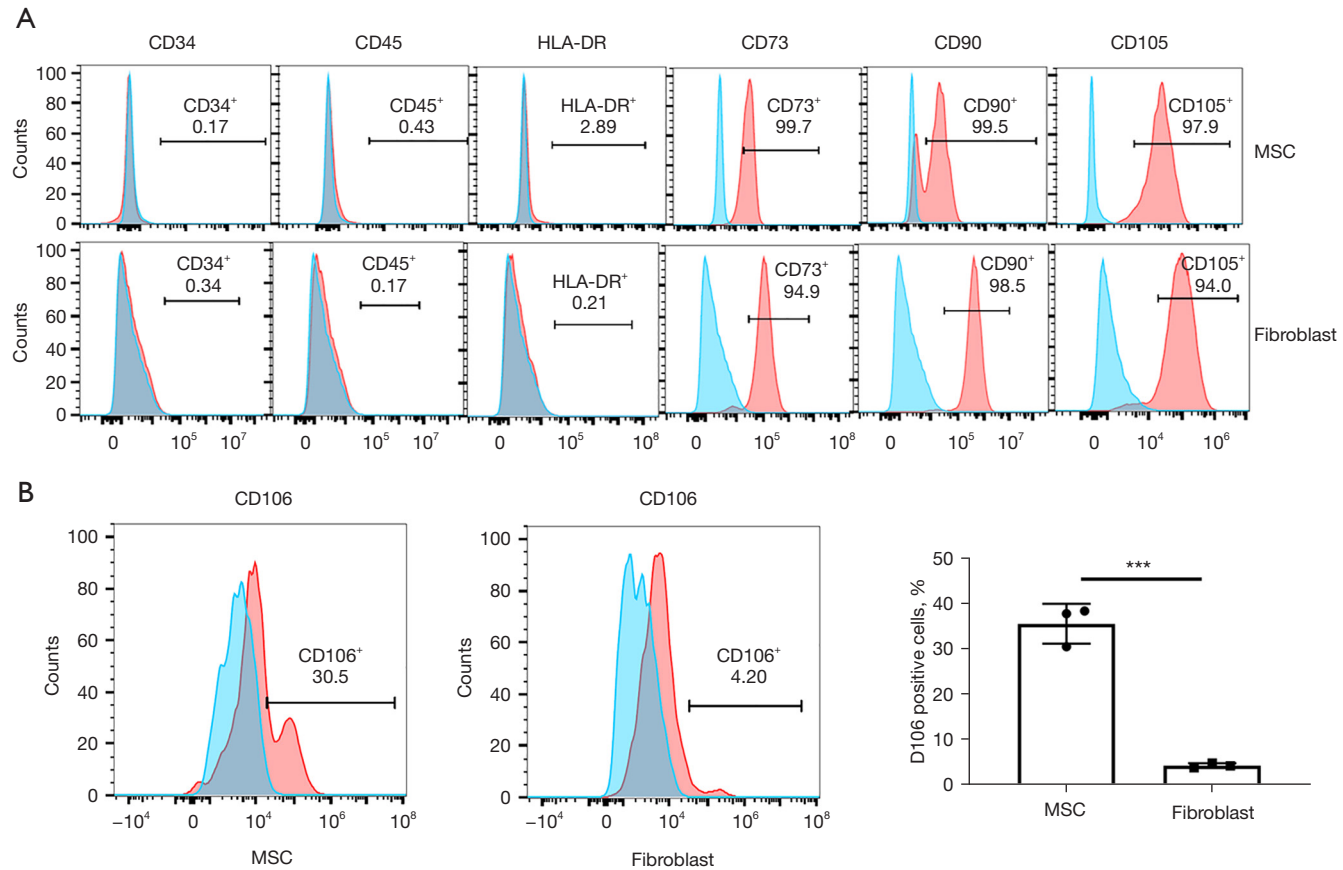

Figure 2 Phenotyping of MSCs and human uterosacral ligament fibroblasts for typical MSC phenotypic markers. (A) Human uterosacral ligament fibroblasts and MSCs were positive for the expression of markers CD90, CD73, and CD105 but negative for CD34, CD45, and HLA-DR in a similar pattern. (B) The positive rate of CD106 in MSCs and in uterosacral ligament fibroblasts. The blue areas represent unstained cells serving as controls; the red areas represent stained cells; the percentages of positively labeled cells are shown. The data shown are the means ± SD of 3 independent experiments. ***, P<0.001. MSC, mesenchymal stem cell; HLA-DR, human leukocyte antigen-DR; SD, standard deviation.

(MMP-1) were significantly different between MSCs and fibroblasts. The expression of COL 1 was higher, and the expression of MMP-1 was lower in CD106$^+$ fibroblasts than in CD106$^-$ fibroblasts. Furthermore, to rule out the possibility that CD106$^+$ fibroblasts are myofibroblasts, the expression of α-smooth muscle actin (α-SMA) was detected, and α-SMA was expressed at lower levels in CD106$^+$ fibroblasts.

CD106 expression decreased in the POP group compared to the non-POP group

We next examined CD106 expression in uterosacral ligament tissue samples. The IHC analysis revealed that CD106$^+$ cells were located around the vessels, and the level of CD106 in the uterosacral ligament of the POP group was considerably lower than that in the non-POP group, as shown by the decreased positive area of the cell membrane (*Figure 6A,6B*). Consistently, flow cytometric analysis confirmed that fibroblasts from patients with POP exhibited a lower percentage of CD106$^+$ cells than those from the non-POP group (*Figure 6C,6D*). These results suggested that the number of CD106$^+$ fibroblasts was reduced in POP uterosacral ligaments compared with the normal uterosacral ligaments.

Discussion

In the present study, we successfully separated CD106$^+$

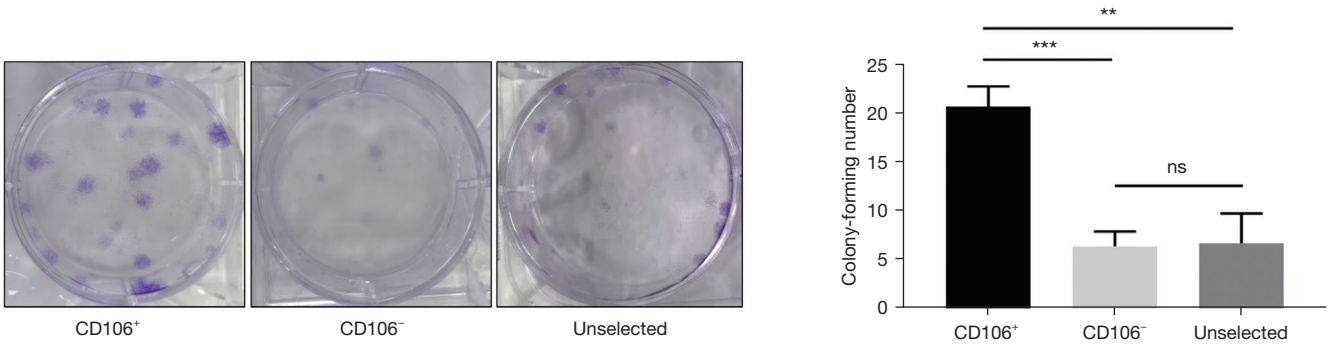

Figure 3 Colony-forming assay of the sorted cell populations and unsorted cells. The colony-forming number of CD106$^+$ fibroblasts was significantly higher than that of CD106$^-$ fibroblasts. There was no difference between CD106$^-$ fibroblasts and unselected cells. Cells were stained with crystal violet after being fixed by 4% paraformaldehyde. The data shown are the means ± SD of 3 independent experiments. **, P<0.01; ***, P<0.001. ns, not significant; SD, standard deviation.

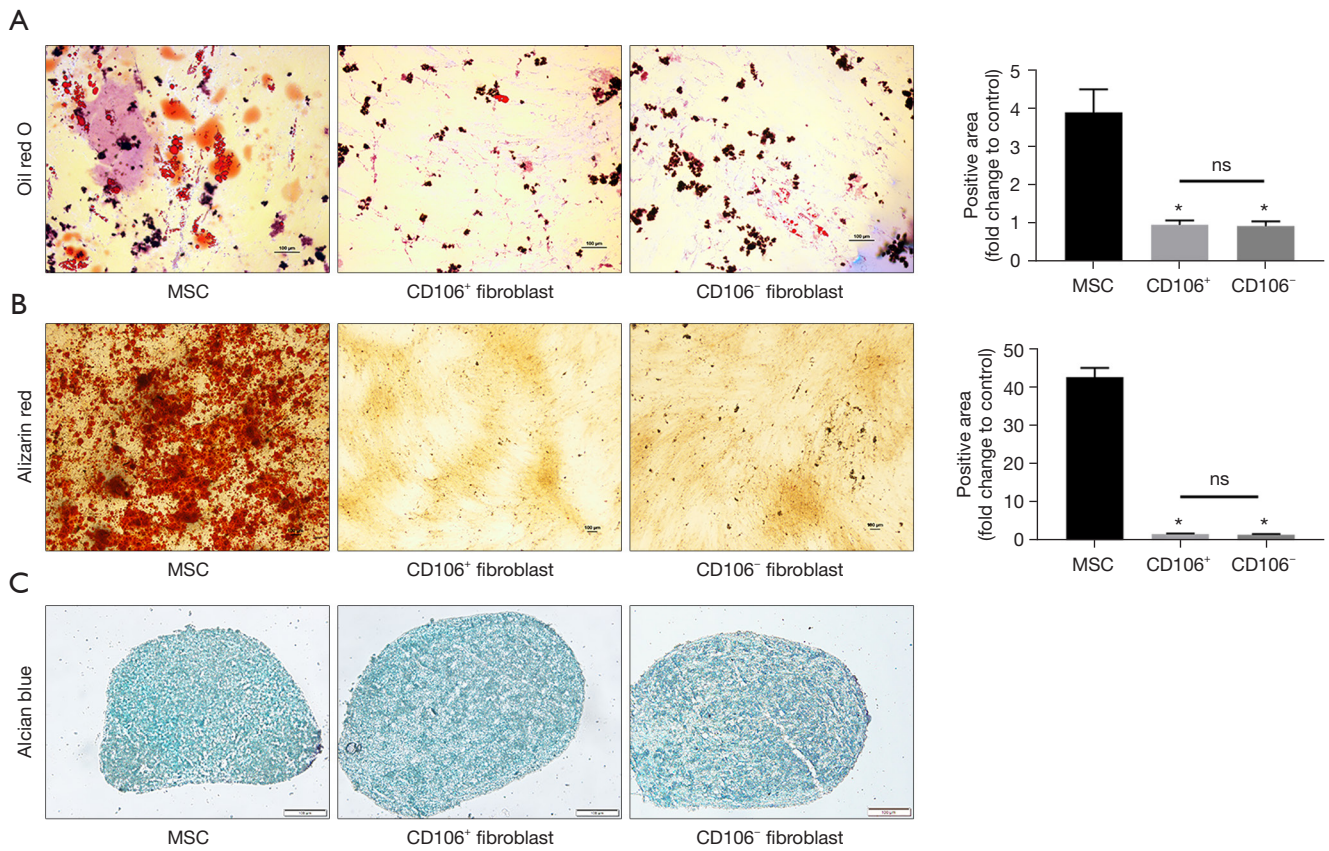

Figure 4 Exploring the trilineage differentiation capacity of MSCs and CD106$^+$ and CD106$^-$ fibroblasts. (A) Adipogenesis was detected by Oil Red O staining. The lipid droplets were quantified by calculating the positive area in each group relative to the control. (B) Osteogenesis was detected by Alizarin Red staining. The mineralized nodules were quantified by calculating the positive area in each group relative to the control. (C) Chondrogenesis was detected by Alcian Blue staining. Fibroblasts incubated in expansion medium served as the controls. Scale bar, 100 μm. The data shown are the means ± SD of 3 independent experiments. *, P<0.05 versus the MSC group. MSC, mesenchymal stem cell; NS, not significant; SD, standard deviation.

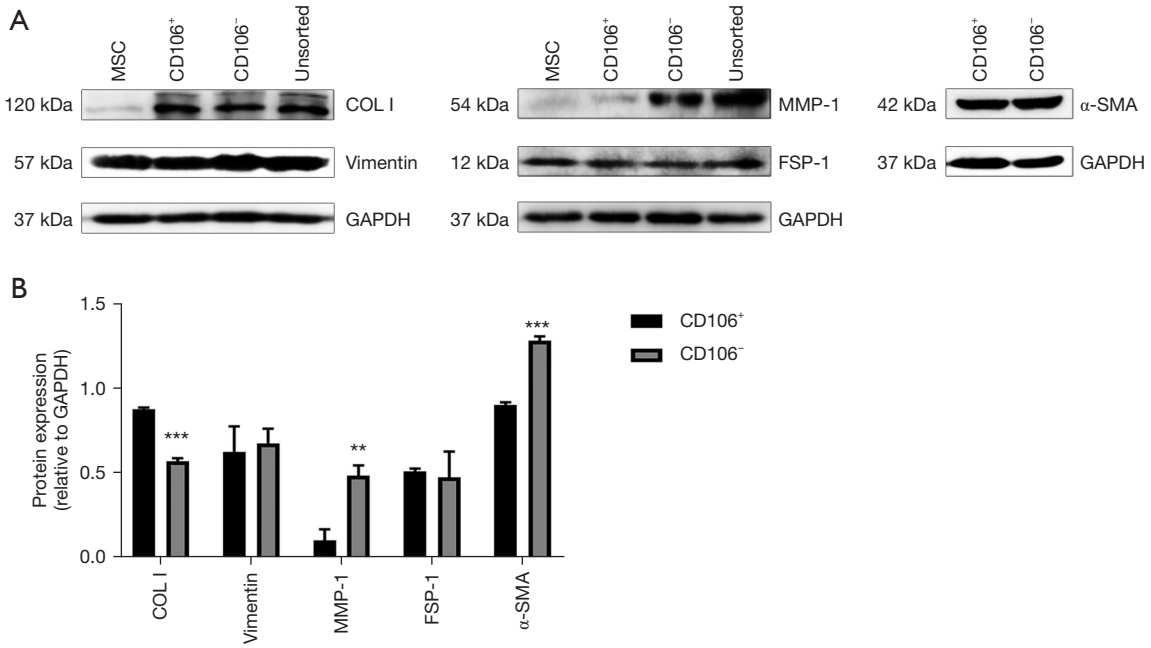

Figure 5 Comparison of the typical fibroblast proteins between CD106$^+$ and CD106$^-$ fibroblasts. (A) A series of typical fibroblast protein levels were determined by western blot analysis in MSCs, CD106$^+$ and CD106$^-$ fibroblasts, and unsorted fibroblasts. (B) Protein densitometric quantification of COL 1, vimentin, MMP-1, FSP-1, and α-SMA. The data shown are the means ± SD of 3 independent experiments. **, P<0.01; ***, P<0.001 versus the CD106$^+$ groups. COL 1, collagen I; GAPDH, glyceraldehyde-3-phosphate dehydrogenase; MMP-1, matrix metallopeptidase-1; FSP-1, fibroblast specific protein-1; α-SMA, α-smooth muscle actin; MSC, mesenchymal stem cell; SD, standard deviation.

and CD106$^-$ fibroblasts and discovered a previously uncharacterized heterogeneity of fibroblasts derived from human uterosacral ligaments (*Figure* 7). The CD106$^+$ fibroblasts possessed a high colony-forming capacity but did not exhibit trilineage differentiation, demonstrating that they were not MSCs. In addition, CD106$^+$ fibroblasts expressed more COL 1 and less MMP-1 and α-SMA than CD106$^-$ fibroblasts. We also investigated the expression levels of CD106 in the POP and non-POP groups and found a significant difference between the 2 groups. These results imply that CD106$^+$ fibroblasts might be a subtype with a high colony-forming ability and different protein expression levels. In addition, a decrease in CD106$^+$ fibroblasts in the uterosacral ligament was shown to be associated with the pathophysiology of POP.

The uterosacral ligament is an essential apical supportive tissue of the uterus, which originates at the S2 to the S4 vertebra and terminates around the dorsal margin of the uterine cervix or the upper third of the posterior vaginal wall (26). Histologically, the uterosacral ligament is a visceral ligament similar to the mesentery structure, which mainly contains connective tissues, vessels, and adipose tissues, and is completely different from skeletal ligaments. As the uterosacral ligament is a primary apical supportive structure of the uterus and vagina, its histological composition has long been studied to better understand the development of POP. Previous studies have found higher levels of MMPs (27) and lower levels of COL 1 (28) in uterosacral ligaments in women with POP than those without POP. Fibroblasts from the uterosacral ligament have been thoroughly investigated to understand the pathophysiological mechanism of POP (29,30).

Fibroblasts represent the most abundant cell type in the uterosacral ligament and other pelvic connective tissues, which help provide mechanical support to pelvic organs. Primary fibroblasts have been isolated from pelvic connective tissues to investigate the pathogenesis of POP (29,30), as their functional changes under mechanical stress or other pathological conditions contribute to the development of POP (8,31). Fibroblasts have been found to exhibit impaired cell contractility (32), reduced cell attachment (33), delayed mechanical

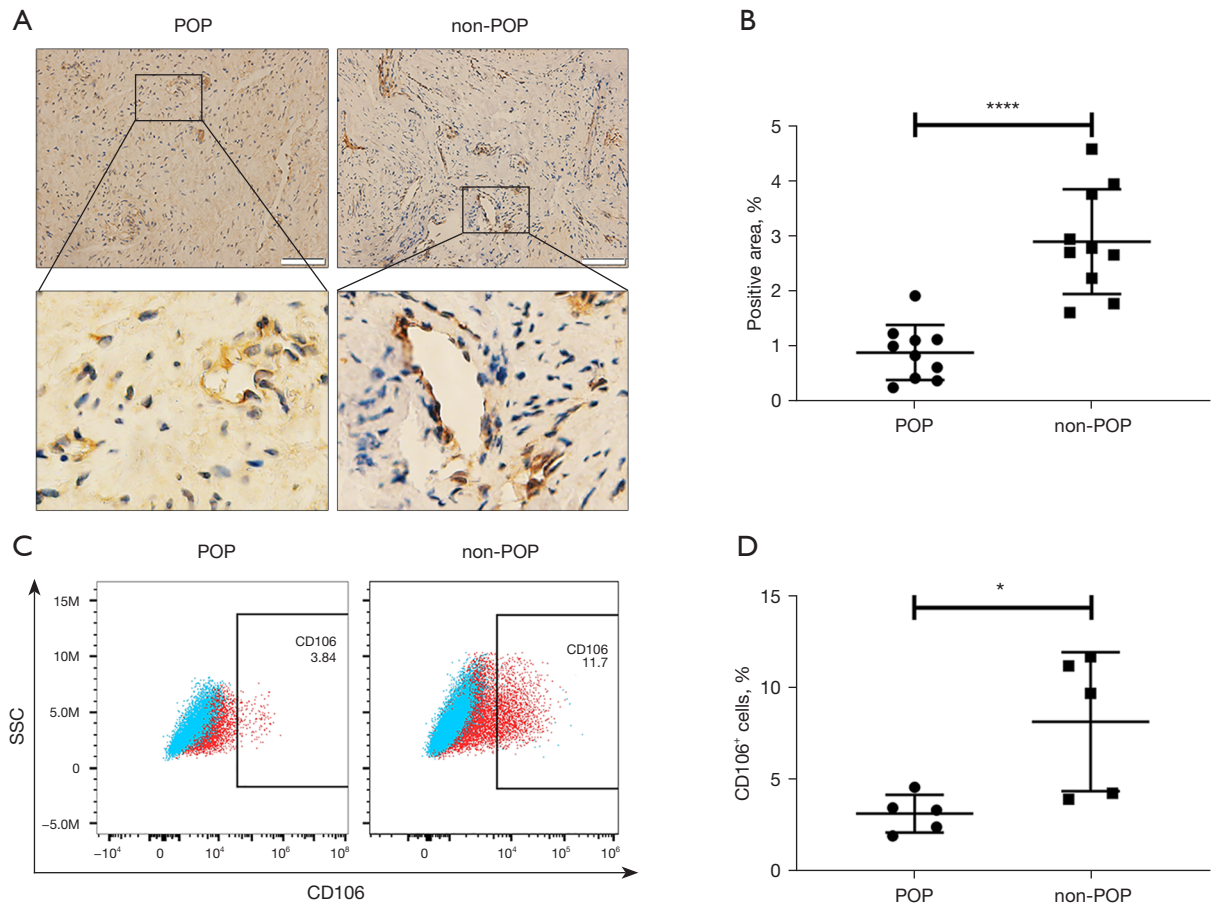

Figure 6 Comparison of CD106 expression between the POP and non-POP groups. (A) IHC analysis of CD106 expression, scale bar, 100 μm. (B) Scatterplot showing the positive area of CD106 in the POP and non-POP groups (n=10). Error bars represent mean ± SD. ****, P<0.0001. (C) Flow cytometry analysis of the CD106$^+$ cells. The blue areas represent unstained cells serving as controls; the red areas represent stained cells; the percentages of positively labeled cells are shown. (D) Scatterplot showing the percentages of CD106$^+$ cells in fibroblasts from the POP and non-POP groups (n=5). Error bars represent mean ± SD. *, P<0.05. POP, pelvic organ prolapse; SSC, side scatter; IHC, immunohistochemistry; SD, standard deviation.

responses (34), increased apoptosis (35), and altered ECM protein production (33) in POP compared to fibroblasts in non-POP. A comprehensive understanding of their phenotypic characteristics, heterogeneity, and specific functions is absent, despite the common use of primary uterosacral ligament fibroblasts. Recently, Li *et al.* (15) reported heterogeneity of vaginal wall fibroblasts by single-cell transcriptome profiling, and 7 distinct subtypes were acquired by sub-clustering. They found that the subtype proportions and gene expression patterns of specific subtypes differed between POP and control groups, demonstrating the importance of further exploring the heterogeneity of fibroblasts to elucidate the pathophysiology of POP. However, the 7 subpopulations were not experimentally validated by quantifying the specific markers of each subtype in POP and non-POP samples, although the single-cell RNA sequencing they used was an efficient approach to reveal cell subpopulations. In addition, the expression profiles and representative markers of each subtype were not presented; thus, we could not speculate which subtype in their report is similar to the CD106$^+$ fibroblasts. In our study, though we did not comprehensively analyze the cellular heterogeneity of the uterosacral ligament, we focused on and characterized the CD106$^+$ fibroblasts, providing more concrete evidence for the heterogeneity of fibroblasts in POP.

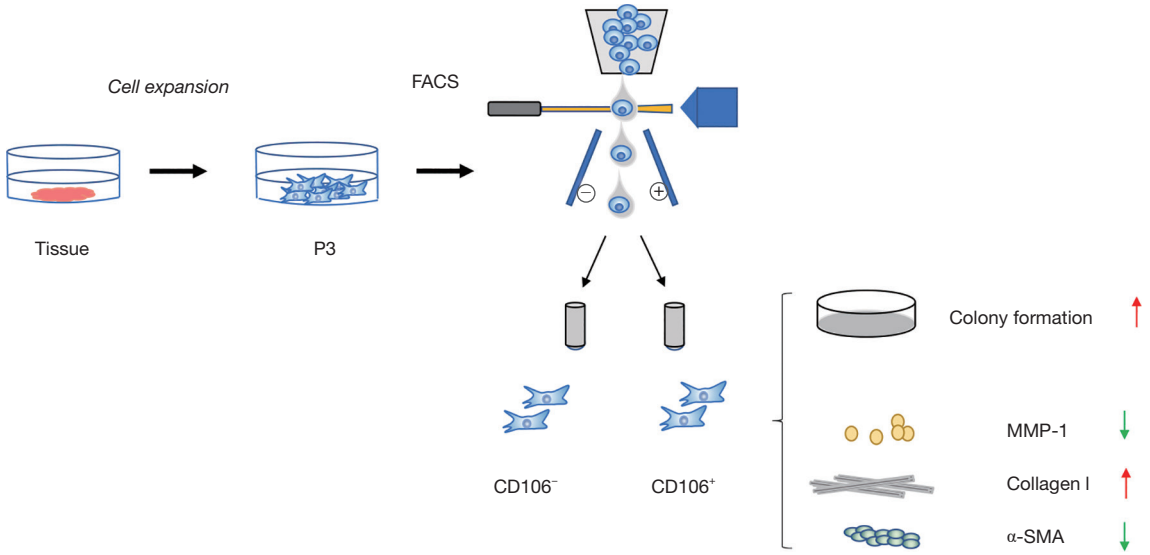

Figure 7 Schematic diagram of the isolation and characteristics of CD106⁺ fibroblasts. The primary fibroblasts isolated from uterosacral ligaments were expanded to passage 3 and then sorted by the surface marker CD106 using FACS. CD106⁺ fibroblasts exhibited a high colony-forming capacity and different protein expressions compared with CD106⁻ fibroblasts. FACS, fluorescence-activated cell sorting; MMP-1, matrix metallopeptidase-1; α-SMA, α-smooth muscle actin.

Currently, CD106 is considered a surface marker of MSCs (17,25,36). Previous studies reported that CD106 was one of the differentially expressed markers between fibroblasts and MSCs (24,25). However, most MSC markers are also expressed on fibroblasts, demonstrating that the 2 cell types are phenotypically indistinguishable (37). This study also found that fibroblasts derived from the uterosacral ligament expressed similar surface markers to BM-MSCs except for CD106. The result was consistent with previous studies reporting that fibroblasts from other organs expressed a similar pattern of surface markers to MSCs. The different expression of CD106 between the uterosacral ligament fibroblasts and MSCs in our study led us to hypothesize that CD106⁺ fibroblasts may be an MSC-like subpopulation of uterosacral ligament fibroblasts. The cell surface proteins CD90, CD73, and CD105 play roles in multiple cellular events and are specific markers of human MSCs. In addition, CD34, CD45, and HLA-DR are markers to exclude cells from the hematopoietic system. The expression pattern of these surface molecules has been a recognized criterion for defining MSCs (38). Previous studies have suggested that CD106⁺ MSCs have enhanced multipotency (19,20) and immunosuppressive activity (17,21,22). A study reported that human CD106⁺ cardiac fibroblasts had enhanced the lymphangiogenesis capacity and improved heart function in post-infarct heart-failure rat models (23). Considering the importance of CD106 for MSCs and the differential expression between MSCs and fibroblasts, we classified CD106⁺ fibroblasts and explored whether they were a novel MSC-like subpopulation in the human uterosacral ligament.

We found that CD106⁺ fibroblasts possessed a high colony-formation capacity but did not exhibit trilineage differentiation, demonstrating that they are not MSCs. A previous study reported that silencing CD106 inhibited the proliferation of human oral squamous carcinoma HN12 cells (39), but the underlying mechanisms of CD106 and its role in cell proliferation are unknown. Another study found that cellular depletion of CD106 inhibited lung fibroblast cell proliferation by reducing the proportion of cells in the G2/M and S phases (40). Our results showed that the protein level of COL 1 increased, while the level of MMP-1 decreased in CD106⁺ fibroblasts, compared with levels in CD106⁻ fibroblasts. The protein levels of vimentin and FSP-1 were not different between CD106⁺ and CD106⁻ fibroblasts, demonstrating that these 2 markers commonly used to identify fibroblasts were expressed conservatively in CD106⁺ fibroblasts. The protein levels of COL 1 and MMP-1 were significantly different between MSCs and fibroblasts, suggesting that the 2 cell types with a similar

surface marker expression could be distinguished by the expression of COL 1 and MMP-1, the former of which is the most abundant protein in pelvic connective tissue, providing the majority of tissue resistance to tension. A decreased content and altered structure of COL 1 are significant pathological alterations in POP (28,41,42). The presence of MMP-1 is essential for the degradation of COL 1, and its expression is increased in POP tissues (4,6,27). Increased collagen degradation in the uterosacral ligament could cause weakening of the tissue and eventually lead to prolapse. In the present study, the protein level of COL 1 increased while the level of MMP-1 decreased in $CD106^+$ fibroblasts compared with $CD106^-$ fibroblasts, suggesting that $CD106^+$ fibroblasts are a protective subpopulation against POP. Furthermore, the differential protein expression results imply that upregulation of the cell number or promoting the cell viability of $CD106^+$ fibroblasts may be a therapeutic strategy for POP.

Myofibroblasts, a differentiated fibroblast population with high proliferation ability, increase secretion of ECM, and at high contraction capacity, are characterized by α-SMA expression (43). Considering the high colony formation capacity and high protein level of COL 1, we detected the protein levels of α-SMA to rule out the possibility that $CD106^+$ fibroblasts are myofibroblasts. The results showed that the expression level of α-SMA in $CD106^+$ fibroblasts was lower than that in $CD106^-$ fibroblasts, which suggested that $CD106^+$ fibroblasts are not myofibroblasts and the cell contraction ability of $CD106^+$ fibroblasts may be weaker than that of $CD106^-$ fibroblasts.

Importantly, we found that the expression of CD106 in the uterosacral ligament tissues of the POP group was considerably downregulated compared with that of the non-POP group. Fibroblasts from patients with POP exhibited lower expression of CD106 than fibroblasts from the non-POP group. Although the sample size was small, this was the first study to confirm a decrease in CD106 protein expression in POP, consistent with the data from 2 previous studies. Both the polymerase chain reaction (PCR) array analysis from Kufaishi *et al.* (33) and the single-cell RNA sequencing results from Li *et al.* (15) indicated that the expression of CD106 decreased in POP compared to in non-POP. However, they did not further verify the results in tissues or cells, and the reasons for the decrease of CD106 in POP are still unknown.

The results of the present study potentially identify a specific subtype of uterosacral ligament fibroblasts, providing a theoretical basis for future investigations on therapies targeting this subpopulation. However, there were some limitations to this study. Future studies should perform RNA sequencing to comprehensively analyze the $CD106^+$ subpopulation, and the culture conditions of the $CD106^+$ fibroblasts need to be improved to inhibit the decline in expression of CD106 after cell propagation. In addition, to understand the roles of the $CD106^+$ subpopulation in the development of POP, the sample size should be larger, and animal studies should be designed to investigate the influence of local injection of $CD106^+$ fibroblasts into the uterosacral ligament.

In conclusion, to our knowledge, this was the first study to report that CD106 identifies a unique subpopulation of uterosacral ligament fibroblasts with high colony-forming capacity and collagen production. The expression of CD106 is reduced in POP, suggesting that a decrease in $CD106^+$ fibroblasts may contribute to the pathogenesis of POP.

Acknowledgments

We acknowledge the work of Jing Zhou from Fudan University, Peng Li from the Hubei Institute of Fine Arts, and Suna Tian from the Hubei Institute of Fine Arts, who have not been listed as authors of this article.

Funding: This work was supported by the National Natural Science Foundation of China (No. 81671439 to YC), the Science and Technology Commission of Shanghai Municipality 2018 YIXUEYINGDAO project (No. 18401902200 to LW), the Science and Technology Innovation Action Plan of Shanghai Natural Science (No. 20ZR1409100 to LW), and the Chinese Association of Integration of Traditional and Western Medicine special foundation for Obstetrics and Gynecology-PuZheng Pharmaceutical Foundation (No. FCK-PZ-08 to LW).

Footnote

Reporting Checklist: The authors have completed the MDAR reporting checklist. Available at https://atm.amegroups.com/article/view/10.21037/atm-21-5136/rc

Data Sharing Statement: Available at https://atm.amegroups.com/article/view/10.21037/atm-21-5136/dss

Conflicts of Interest: All authors have completed the ICMJE uniform disclosure form (available at https://atm.amegroups.com/article/view/10.21037/atm-21-5136/coif). The authors have no conflicts of interest to declare.

Ethical Statement: The authors are accountable for all aspects of the work in ensuring that questions related to the accuracy or integrity of any part of the work are appropriately investigated and resolved. All procedures performed in this study involving human participants were in accordance with the Declaration of Helsinki (as revised in 2013). The study was approved by the Ethics Committee of the Obstetrics and Gynecology Hospital of Fudan University (No. 2017-12) and informed consent was taken from all the patients.

References

1. Barber MD, Maher C. Epidemiology and outcome assessment of pelvic organ prolapse. Int Urogynecol J 2013;24:1783-90.
2. Vergeldt TF, Weemhoff M, IntHout J, et al. Risk factors for pelvic organ prolapse and its recurrence: a systematic review. Int Urogynecol J 2015;26:1559-73.
3. Kieserman-Shmokler C, Swenson CW, Chen L, et al. From molecular to macro: the key role of the apical ligaments in uterovaginal support. Am J Obstet Gynecol 2020;222:427-36.
4. Dviri M, Leron E, Dreiher J, et al. Increased matrix metalloproteinases-1,-9 in the uterosacral ligaments and vaginal tissue from women with pelvic organ prolapse. Eur J Obstet Gynecol Reprod Biol 2011;156:113-7.
5. Alarab M, Bortolini MA, Drutz H, et al. LOX family enzymes expression in vaginal tissue of premenopausal women with severe pelvic organ prolapse. Int Urogynecol J 2010;21:1397-404.
6. Gong R, Xia Z. Collagen changes in pelvic support tissues in women with pelvic organ prolapse. Eur J Obstet Gynecol Reprod Biol 2019;234:185-9.
7. Hong S, Li H, Wu D, et al. Oxidative damage to human parametrial ligament fibroblasts induced by mechanical stress. Mol Med Rep 2015;12:5342-8.
8. Marcu RD, Mischianu DLD, Iorga L, et al. Oxidative Stress: A Possible Trigger for Pelvic Organ Prolapse. J Immunol Res 2020;2020:3791934.
9. Zhang L, Dai F, Chen G, et al. Molecular mechanism of extracellular matrix disorder in pelvic organ prolapses. Mol Med Rep 2020;22:4611-8.
10. Liu C, Yang Q, Fang G, et al. Collagen metabolic disorder induced by oxidative stress in human uterosacral ligament derived fibroblasts: A possible pathophysiological mechanism in pelvic organ prolapse. Mol Med Rep 2016;13:2999-3008.
11. Rinkevich Y, Walmsley GG, Hu MS, et al. Skin fibrosis. Identification and isolation of a dermal lineage with intrinsic fibrogenic potential. Science 2015;348:aaa2151.
12. Saraswati S, Marrow SMW, Watch LA, et al. Identification of a pro-angiogenic functional role for FSP1-positive fibroblast subtype in wound healing. Nat Commun 2019;10:3027.
13. Xie T, Wang Y, Deng N, et al. Single-Cell Deconvolution of Fibroblast Heterogeneity in Mouse Pulmonary Fibrosis. Cell Rep 2018;22:3625-40.
14. Matsushima S, Aoshima Y, Akamatsu T, et al. CD248 and integrin alpha-8 are candidate markers for differentiating lung fibroblast subtypes. BMC Pulm Med 2020;20:21.
15. Li Y, Zhang QY, Sun BF, et al. Single-cell transcriptome profiling of the vaginal wall in women with severe anterior vaginal prolapse. Nat Commun 2021;12:87.
16. Alon R, Kassner PD, Carr MW, et al. The integrin VLA-4 supports tethering and rolling in flow on VCAM-1. J Cell Biol 1995;128:1243-53.
17. Yang ZX, Han ZB, Ji YR, et al. CD106 identifies a subpopulation of mesenchymal stem cells with unique immunomodulatory properties. PLoS One 2013;8:e59354.
18. Honczarenko M, Le Y, Swierkowski M, et al. Human bone marrow stromal cells express a distinct set of biologically functional chemokine receptors. Stem Cells 2006;24:1030-41.
19. Gronthos S, Zannettino AC, Hay SJ, et al. Molecular and cellular characterisation of highly purified stromal stem cells derived from human bone marrow. J Cell Sci 2003;116:1827-35.
20. Fujita R, Tamai K, Aikawa E, et al. Endogenous mesenchymal stromal cells in bone marrow are required to preserve muscle function in mdx mice. Stem Cells 2015;33:962-75.
21. Ren G, Zhao X, Zhang L, et al. Inflammatory cytokine-induced intercellular adhesion molecule-1 and vascular cell adhesion molecule-1 in mesenchymal stem cells are critical for immunosuppression. J Immunol 2010;184:2321-8.

22. Castro-Manrreza ME, Montesinos JJ. Immunoregulation by mesenchymal stem cells: biological aspects and clinical applications. J Immunol Res 2015;2015:394917.
23. Iwamiya T, Segard BD, Matsuoka Y, et al. Human cardiac fibroblasts expressing VCAM1 improve heart function in postinfarct heart failure rat models by stimulating lymphangiogenesis. PLoS One 2020;15:e0237810.
24. Soundararajan M, Kannan S. Fibroblasts and mesenchymal stem cells: Two sides of the same coin? J Cell Physiol 2018;233:9099-109.
25. Halfon S, Abramov N, Grinblat B, et al. Markers distinguishing mesenchymal stem cells from fibroblasts are downregulated with passaging. Stem Cells Dev 2011;20:53-66.
26. Ramanah R, Berger MB, Parratte BM, et al. Anatomy and histology of apical support: a literature review concerning cardinal and uterosacral ligaments. Int Urogynecol J 2012;23:1483-94.
27. Usta A, Guzin K, Kanter M, et al. Expression of matrix metalloproteinase-1 in round ligament and uterosacral ligament tissue from women with pelvic organ prolapse. J Mol Histol 2014;45:275-81.
28. Yucel N, Usta A, Guzin K, et al. Immunohistochemical analysis of connective tissue in patients with pelvic organ prolapse. J Mol Histol 2013;44:97-102.
29. Zhao X, Liu L, Li R, et al. Hypoxia-Inducible Factor 1-α (HIF-1α) Induces Apoptosis of Human Uterosacral Ligament Fibroblasts Through the Death Receptor and Mitochondrial Pathways. Med Sci Monit 2018;24:8722-33.
30. Wang X, Wang X, Zhou Y, et al. Mitofusin2 regulates the proliferation and function of fibroblasts: The possible mechanisms underlying pelvic organ prolapse development. Mol Med Rep 2019;20:2859-66.
31. Huang L, Zhao Z, Wen J, et al. Cellular senescence: A pathogenic mechanism of pelvic organ prolapse (Review). Mol Med Rep 2020;22:2155-62.
32. Ruiz-Zapata AM, Kerkhof MH, Zandieh-Doulabi B, et al. Functional characteristics of vaginal fibroblastic cells from premenopausal women with pelvic organ prolapse. Mol Hum Reprod 2014;20:1135-43.
33. Kufaishi H, Alarab M, Drutz H, et al. Comparative Characterization of Vaginal Cells Derived From Premenopausal Women With and Without Severe Pelvic Organ Prolapse. Reprod Sci 2016;23:931-43.
34. Ruiz-Zapata AM, Kerkhof MH, Zandieh-Doulabi B, et al. Fibroblasts from women with pelvic organ prolapse show differential mechanoresponses depending on surface substrates. Int Urogynecol J 2013;24:1567-75.
35. Zeng W, Li Y, Li B, et al. Mechanical Stretching induces the apoptosis of parametrial ligament Fibroblasts via the Actin Cytoskeleton/Nr4a1 signalling pathway. Int J Med Sci 2020;17:1491-8.
36. Yang YK, Ogando CR, Wang See C, et al. Changes in phenotype and differentiation potential of human mesenchymal stem cells aging in vitro. Stem Cell Res Ther 2018;9:131.
37. Denu RA, Nemcek S, Bloom DD, et al. Fibroblasts and Mesenchymal Stromal/Stem Cells Are Phenotypically Indistinguishable. Acta Haematol 2016;136:85-97.
38. Dominici M, Le Blanc K, Mueller I, et al. Minimal criteria for defining multipotent mesenchymal stromal cells. The International Society for Cellular Therapy position statement. Cytotherapy 2006;8:315-7.
39. Sun L, Liu L, Yu T, et al. VCAM1-targeted RNA interference inhibits the proliferation of human oral squamous carcinoma HN12 cells. Oncol Lett 2018;15:5650-4.
40. Agassandian M, Tedrow JR, Sembrat J, et al. VCAM-1 is a TGF-β1 inducible gene upregulated in idiopathic pulmonary fibrosis. Cell Signal 2015;27:2467-73.
41. Vulic M, Strinic T, Tomic S, et al. Difference in expression of collagen type I and matrix metalloproteinase-1 in uterosacral ligaments of women with and without pelvic organ prolapse. Eur J Obstet Gynecol Reprod Biol 2011;155:225-8.
42. Salman MC, Ozyuncu O, Sargon MF, et al. Light and electron microscopic evaluation of cardinal ligaments in women with or without uterine prolapse. Int Urogynecol J 2010;21:235-9.
43. Hinz B, Phan SH, Thannickal VJ, et al. The myofibroblast: one function, multiple origins. Am J Pathol 2007;170:1807-16.

Cite this article as: Sima Y, Li J, Xiao C, Xu L, Wang L, Chen Y. CD106/VCAM-1 distinguishes a fibroblast subpopulation with high colony-forming capacity and distinct protein expression from the uterosacral ligament. Ann Transl Med 2022;10(9):511. doi: 10.21037/atm-21-5136

